



OPEN ACCESS

EDITED BY

Carlos Eduardo Fonseca-Alves,
Paulista University, Brazil

REVIEWED BY

Valeria Grieco,
University of Milan, Italy
Pedro Luiz Porfirio Xavier,
University of São Paulo, Brazil

*CORRESPONDENCE

Dasa Cizkova
✉ dasa.cizkova@uvlf.sk

RECEIVED 24 June 2025

REVISED 08 December 2025

ACCEPTED 15 December 2025

PUBLISHED 28 January 2026

CITATION

Nosalova N, Huniadi M, Valencakova A,
Hornakova L, Kalinaj B, Almasiova V,
Marcincakova D, Kubatka P, Hornak S and
Cizkova D (2026) Establishment and
characterization of primary epithelial cell
cultures from healthy canine mammary gland
tissue.

Front. Vet. Sci. 12:1652991.

doi: 10.3389/fvets.2025.1652991

COPYRIGHT

© 2026 Nosalova, Huniadi, Valencakova,
Hornakova, Kalinaj, Almasiova, Marcincakova,
Kubatka, Hornak and Cizkova. This is an
open-access article distributed under the
terms of the [Creative Commons Attribution
License \(CC BY\)](https://creativecommons.org/licenses/by/4.0/). The use, distribution or
reproduction in other forums is permitted,
provided the original author(s) and the
copyright owner(s) are credited and that the
original publication in this journal is cited, in
accordance with accepted academic
practice. No use, distribution or reproduction
is permitted which does not comply with
these terms.

Establishment and characterization of primary epithelial cell cultures from healthy canine mammary gland tissue

Natalia Nosalova¹, Mykhailo Huniadi¹, Alexandra Valencakova¹,
Lubica Hornakova¹, Blazej Kalinaj¹, Viera Almasiova²,
Dana Marcincakova³, Peter Kubatka¹, Slavomir Hornak¹ and
Dasa Cizkova^{1,4*}

¹Small Animal Clinic, University of Veterinary Medicine and Pharmacy in Košice, Košice, Slovakia, ²Department of Anatomy, Histology and Physiology, University of Veterinary Medicine and Pharmacy in Košice, Košice, Slovakia, ³Department of Pharmacology and Toxicology, University of Veterinary Medicine and Pharmacy in Košice, Košice, Slovakia, ⁴Institute of Neuroimmunology, SAS, Bratislava, Slovakia

Introduction: In regenerative medicine and comparative oncology, the development of physiologically relevant in vitro models is critical for advancing our understanding of tissue homeostasis, cellular differentiation, and early tumorigenesis. Such models provide controlled experimental systems to investigate normal mammary gland function, assess responses to therapeutic agents, and establish baseline characteristics for distinguishing healthy from pathological tissue.

Methods: This study successfully established and characterized primary epithelial cell cultures derived from histologically normal canine mammary gland (CMG) tissue. Samples from two healthy female dogs were obtained during elective ovariectomy. Following enzymatic digestion and optimized culture conditions, isolated cells adhered within 24 hours and reached confluence within 6–7 days, maintaining over 95% viability.

Results and discussion: Histological analysis confirmed either active lactational or regressive tissue states. Cell growth and metabolic activity were evaluated using the CELLigence system and XTT assay, with optimal results achieved at a seeding density of 4,000 cells per well. Immunofluorescence staining confirmed epithelial identity (pan-CK, CK8/18), apical MUC1 expression, low Ki-67 levels and negative expression of mesenchymal markers (vimentin, S100), indicating a healthy, non-cancerous cell population with moderate proliferative activity. This study provides the first detailed protocol for establishing primary CMG epithelial cultures and validates their suitability as a reference model for future oncological studies. Overall, this platform supports translational research, including drug testing and biomarker discovery, contributes to personalized veterinary therapies and enhanced understanding of mammary gland pathology in both dogs and humans.

KEYWORDS

biomarkers, canine mammary gland, histology, isolation of cells, oncology, primary cell cultures

1 Introduction

The active mammary gland is a compound, tubuloalveolar gland found only in mammals, designed to feed the offspring and support its immune system (1). Glandular parenchyma consists of alveoli and ductal structures organized into lobules, which are surrounded by connective tissue septa. The ductal system begins with an intralobular duct, which drains into an interlobular duct and finally into lactiferous ducts. Several lactiferous ducts drain into a lactiferous sinus, which joins the teat sinus (2). The mammary gland is highly dependent on hormonal stimulation, and its development and action are controlled by various hormones (prolactin, estrogen, and progesterone). The mammary gland is also strongly influenced by the estrous cycle and pregnancy (1). The mammary gland of women and dogs share similar morphological characteristics, differing in the number of glandular units, number of nipples/teats, hormonal regulation, functional cycles and milk composition. In dogs, four to six pairs of glands have been described, with the inguinal pairs being the largest, the abdominal pairs intermediate, and the thoracic pairs the smallest in size (1).

Due to the constantly increasing number of cases and the clinical significance of breast cancer (BC), research into physiology and pathology of mammary glands has increased significantly. In this context, female dogs have emerged as valuable comparative animal models for studying human cancer, providing samples for the development of alternative *in vitro* models and playing a key role in advancing progress in this research area (3). Building on tissue-derived cell cultures, established cell lines play a fundamental role in research for their importance in the study of diseases, stem and cancer cells investigation, drug discovery, and the establishment of new therapies (4). Even though immortalized cell lines are widely employed in biomedical research because of their reproducibility and ease of maintenance, they often differ greatly from *in vivo* cells, exhibiting altered gene expression profiles and the loss of tissue-specific functions (5). For these reasons, primary cell cultures isolated from tissues are becoming more widely acknowledged as more physiologically relevant models in molecular biology, oncology and pharmacological research (6). Furthermore, they serve as an excellent preclinical model essential for studying gene expression, modification of signaling pathways, oncogene activation, and the development of new drugs and therapeutic strategies (7). Several cell types can be isolated from the canine mammary gland, including epithelial cells, myoepithelial cells, stromal fibroblasts, adipocytes, mesenchymal stem cells (MSCs), and resident immune cells (1, 3, 4, 7, 8). Among these, primary cultures of mammary epithelial cells are the most commonly used in research because of their importance in studying gland development, hormonal regulation, lactation physiology, and neoplastic transformation (4, 8). These cultures serve as essential reference models for investigating basic physiological processes such as proliferation, hormonal interactions and differentiation. In the context of cancer research, they allow for direct comparison with tumor cells, assisting to identify cancer specific alterations. Additionally, they are invaluable for assessing treatment methods and play a key role in the development and validation of diagnostic and prognostic markers for canine mammary tumors (8, 9).

In line with this, the present study aimed to establish and characterize primary epithelial cell cultures from healthy canine mammary gland (CMG) tissue as a relevant *in vitro* model for studying normal mammary biology and early neoplastic

transformation. Key objectives included: confirming the physiological status of donor tissue via histology; assessing cell morphology, adherence, and proliferation using xCELLigence and XTT assays; and verifying epithelial identity through immunofluorescence staining (pan-CK, CK8/18, MUC1, Ki-67). By optimizing growth conditions and validating cell phenotypes, the study provides a foundation for developing standardized cell lines to support comparative oncology and personalized veterinary therapies.

2 Materials and methods

2.1 Animals and tissue samples

At the beginning of the experiment, informed consent was obtained from the owners of the animals to collect biological material. The research protocols were approved by the ethics committee of the UVMP in Košice (EKVP/2023–02). The tissue donors were two female dogs, an 8-year-old French Bulldog (C1) with a weight of approximately 9 kg and a 1-year-old Dachshund (C2) with a weight of 7.7 kg. The collection of healthy mammary gland tissue (n = 2) was performed during preventive ovariohysterectomy at Small Animal Clinic UVMP in Košice according to the standard veterinary procedures under strict sterile conditions. After surgical excision, the tissue sample (approx. 1 cm³) was transported to the laboratory in a sterile solution consisting of 1x phosphate-buffered saline (PBS, Sigma, United States) supplemented with 0.02% gentamicin solution (50 mg/mL, Sigma, USA). The tissue was mechanically divided into smaller pieces under sterile conditions. A portion of the tissue was transferred into PBS containing gentamicin (0.02%) for subsequent cell isolation. Smaller fragments of glandular tissue (approx. 0.5 cm³) were immediately fixed in 4% formaldehyde to preserve the tissue architecture for histological and immunohistochemical analysis.

2.2 Isolation of primary cell cultures

The isolation of primary cell cultures was performed in a Biosafety Cabinets (Herasafe, Class II Biological Safety Cabinet, Thermo Fisher Scientific Inc., United States, BioSafe, Class II, A2, Ekokrok, SK) under sterile conditions to prevent contamination by unwanted pathogens. The canine mammary gland tissue immersed in PBS was first mechanically dissociated using surgical instruments. Then enzymatic digestion was performed with 1 mg/mL collagenase IV (Gibco, Invitrogen, Carlsbad, CA, United States) in Earle's Balanced Salts Solution (Biosera, France) supplemented by 1% Antibiotic/Antimycotic solution (ATB/ATM, 1% solution of penicillin (10,000 U/mL), streptomycin (10,000 µg/mL), and amphotericin B (25 µg/mL) Sigma, United States) and 0.1% gentamicin. After 45 min of incubation at 37 °C, the enzyme was neutralized with the same volume of fetal bovine serum (FBS, Sigma, United States). The digested tissue was filtered through a cell strainer with the size of 100 µL and centrifuged at 1200 rpm/ 7 min. The cell pellet was resuspended in 1 mL of culture medium Dulbecco's modified Eagle's medium High Glucose (DMEM HG, Sigma, CA, United States). The cells were plated on a 25 cm² tissue culture flask/T25 (Corning, Lowell, MA, United States) and maintained in a humidified atmosphere containing 5% CO₂ at 37 °C.

2.3 Morphology, cultivation, and cryopreservation of primary cell cultures

CMG cells were cultivated in DMEM HG supplemented with 10% FBS, 2% ATB/ATM solution, 0.1% gentamicin, and 1% L-glutamine (Sigma, United States) under standard culture conditions (5% CO₂ at 37 °C) until the formation of a monolayer. The medium was changed every 2–3 days of incubation. The adherence properties, morphology and expansion capacity of CMG cells were evaluated after 24, 48, and 72 h of cultivation using the inverted microscope Zeiss Axiovert 200 equipped with a digital acquisition system. When the cell confluence reached 80–90%, primary culture cells were subcultured to establish passage 1 (P1). The CMG cells were washed with PBS and detached from the bottom of the culture flask using 1 mL of 0.05% trypsin/EDTA solution (Sigma, CA, United States). After incubation for 3–5 min at 37 °C, the enzyme was deactivated with the same volume of FBS. The suspension of cells was centrifuged at 1200 rpm/7 min. The supernatant was removed, and 1 mL of DMEM HG was added for resuspension of the cell pellet. Afterward, the cells were counted in a trypan blue 4% solution using a hemocytometer under an inverted microscope. For the counting of the total number of cells, the calculation formula was used: Total number of cells/ml = (Number of viable cells × dilution factor × 10⁴) / (Number of squares counted). The percentage of viable cells was calculated as (the number of viable cells / total number of cells) × 100. The part of the pellet was plated on a 75 cm² tissue culture flask/T75 cm² (Corning, Lowell, MA, United States) for further experiments. The rest of the cell pellet was centrifuged (1,200 rpm/7 min) and resuspended in freezing medium composed of 50% DMEM HG, 40% FBS and 10% dimethyl sulfoxide (DMSO, Sigma, United States). The cells in cryogenic vials (Ratiolab, Deutschland) were frozen at 1 °C/min in MrFrosty Freezing Container (Sigma, USA) in 80 °C for 24 h and subsequently stored in liquid nitrogen.

2.4 Growth assay

The growth curve of cultured cells was evaluated using the xCELLigence system, Real-Time Cell Analyzer (RTCA, Roche Applied Sciences, Mannheim, Germany) and XTT assay.

The RTCA is a system that relies on electronic detection to monitor biological processes. The RTCA uses E-plates (Acea Bioscience, San Diego, CA, United States) equipped with gold microelectrodes on the surface of the culture plate. These electrodes measure electrical impedance, which allows the system to detect changes in cell properties, such as their adherence, changes in morphology, or proliferation (10). All the changes are expressed as cell index (CI) and recorded in curves. The CMG cells at passage 1 (P1) were seeded into 96-well E-plates at different concentrations of cells, 1 × 10³, 2 × 10³, 4 × 10³, and 8 × 10³ cells per well in 200 µL of DMEM HG supplemented with 2% ATB/ATM solution, in triplicate, and cultured at 37 °C and 5% CO₂ for a total of 100 h. The results were experimentally evaluated following the manufacturer's instructions for the xCELLigence Real-Time Cell Analyzer (RTCA, ACEA Biosciences, United States).

XTT assay is used for the detection of viable, metabolically active cells, which can reduce yellow XTT dye into orange formazan. The cells (P1) were seeded in a 96-well plate at the same concentrations as those used for the xCELLigence assay, in 100 µL of DMEM

HG. After three incubation times (24, 48, and 72 h), 50 µL of freshly prepared XTT solution, composed of XTT labeling reagent and electron coupling reagent in a ratio 50:1, was added to the wells. The plates were incubated at 37 °C and 5% CO₂ for 4 h. The absorbance was measured at a wavelength of 450 nm using the APOLLO Absorbance Reader (Berthold Systems, United States) to analyze cell viability.

2.5 Sample preparation for light microscopy evaluation

The tissue samples were immersed in 4% formaldehyde, then dehydrated through a graded series of ethanol (50, 70, 100%), transferred to xylene, and embedded in Paraplast blocks (Sigma-Aldrich). Serial sections (*n* = 6), 6 µm thick obtained from each block were stripped of paraplast and stained using a routine hematoxylin and eosin (H&E) method. Sections were evaluated using a Zeiss Axio Lab A1 light microscope and photodocumented using an Axio Cam ERc 5 camera. Twenty (11) randomly selected fields of each tissue section were evaluated by two independent histologists.

2.6 Immunocytochemistry

CMG cells (P2) were seeded on round coverslips (diameter = 12 mm) placed in 24-well plates (1.5 × 10⁴ cells / well) in a final volume of 500 µL. After reaching confluency (4 days), cells were washed with PBS and fixed with 4% paraformaldehyde (pH = 7.2) for 20 min at room temperature. Following fixation, CMG cells were washed again with PBS and incubated in a solution of 10% normal goat serum (NGS) in PBS supplemented with 0.2% Triton X-100 (PBS TX100) for 1 h at room temperature. This process ensures better access of the antibody to intracellular proteins and minimizes non-specific binding. Primary antibodies (Table 1) diluted in PBS TX100 were added to the cells for 24 h at 4 °C. The following day, CMG cells were washed with PBS and incubated with the appropriate secondary antibodies (Table 1) diluted in PBS TX100 for 1 h at room temperature in the dark. During this step, DAPI (1:200) was also added to the cells to stain nuclei. Lastly, cells were washed with PBS three times for 5 min. Coverslips were mounted to the slides using Vectashield mounting medium (Cole-Parmer, Vernon Hills, IL, United States) and analyzed by a Zeiss AxioVision-APOTOM fluorescence microscope. Negative controls were prepared by excluding the primary antibodies from the staining procedure.

2.7 Immunohistochemistry

For immunohistochemistry, samples were prepared similarly to the (H&E) staining. The sections were stripped of paraplast and antigen retrieval was carried out with 10 mM citrate buffer (pH = 6) for 10 min at 97 °C, followed by washing with PBS. Then, incubation with 10% NGS, primary and secondary antibodies (Table 1) was performed by the same methodological procedure as for immunocytochemical staining described above. Vectashield medium was used to mount coverslips to the slides. The stained sections were evaluated using a Zeiss AxioVision-APOTOM fluorescence microscope.

TABLE 1 List of antibodies used for immunofluorescence staining of cells and tissues.

Primary antibodies			
Name	Catalog number	Dilution	Manufacturer
Ki-67, RBX-500 UL	ab15580	1:300	Abcam
Mouse Cytokeratin, pan mAb (AE-1/AE-3)	NBP2-29429	1:100	Biotechne
Mouse mAb anti-Cytokeratin 8/18 (5D 3)	NB120-17139	1:100	
Mouse anti-MUC1 (OT12E3)	NBP2-45838	1:200	
Flex Polyclonal Rabbit Anti-S100	IR504	1:200	Dako
Vimentin Monoclonal Antibody (V9)	MA5-11883	1:250	Invitrogen

Secondary antibodies			
Name	Catalog number	Dilution	Manufacturer
Alexa Fluor™ 488 Goat anti-Rabbit IgG (H + L)	A-11034	1:200	Invitrogen
Alexa Fluor™ 488 Goat anti-Mouse IgG (H + L)	A-11001	1:200	
Alexa Fluor™ 594 Goat anti-Mouse IgG (H + L)	A-11032	1:200	
Alexa Fluor™ 594 Goat anti-Rabbit IgG (H + L)	A-11037	1:200	

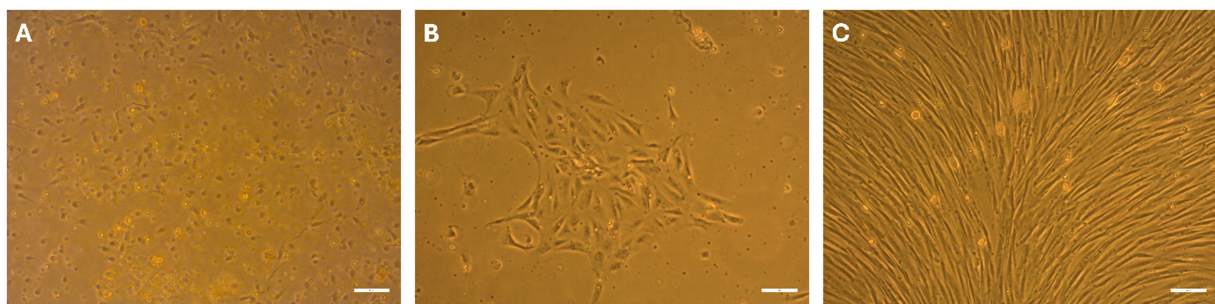


FIGURE 1

Morphological development of primary CMG cells. Phase-contrast images show CMG cells at passage 0 (P0) on day *in vitro* (DIV) 1 (A), DIV 2 (B), and DIV 7 (C). Cells exhibited initial adherence and polygonal morphology by DIV 1, progressing to fibroblast-like shape (DIV 2) with increased confluence and organization into a monolayer by DIV 7. Scale bars: 50 μ m.

3 Results

3.1 General features of primary canine mammary gland cells

With the protocol established herein, primary cells from canine mammary gland tissue were isolated by enzymatic digestion and plated in a culture flask (T25) under standard conditions. The yield of isolated cells was approximately 1×10^6 cells/mL. By the following day, part of the cells had already adhered and changed their shape to a polygonal one. Some rounded precursor cells with light cytoplasm were still actively divided (Figure 1A). At 48 h post-plating, the first medium change was performed, and the cells showed a good attachment to the surface, displaying polygonal and fibroblast-like shapes (Figure 1B). The non-attached material, composed of degenerated cells and detritus, was washed away. After 6–7 days, the monolayers were confluent (Figure 1C), and the CMG cells were subcultured without losing their proliferative properties. Cell viability before each experiment was greater than 95%.

3.2 Histological evaluation of canine mammary gland tissue

The mammary gland of the female dog (C1) (French Bulldog breed) during active lactation consisted of large lobules separated by connective tissue septa. Each lobule contained very well-developed secretory units, alveoli and tubules, which were surrounded by a sparse loose connective tissue-*interstitium* with small blood vessels. Alveoli, ranging from spherical to ovoid shape and elongated tubules were lined with tall, simple cuboidal secretory epithelium. Lactiferous content was observed in the lumens of both tubules and alveoli. Within the lobules, small intralobular ducts lined by low, simple cuboidal epithelium were found. Septa separating individual lobules contained very well-developed interlobular ducts with large, irregular lumens filled with secretory product/milk (Figures 2A,B).

In the second dog (C2) (Dachshund), the mammary gland was in regression state, and its secretory alveoli and tubules were irregularly shaped, shrunken, and often with completely collapsed lumens. Some alveoli still contained secretory product/milk. The interlobular ducts

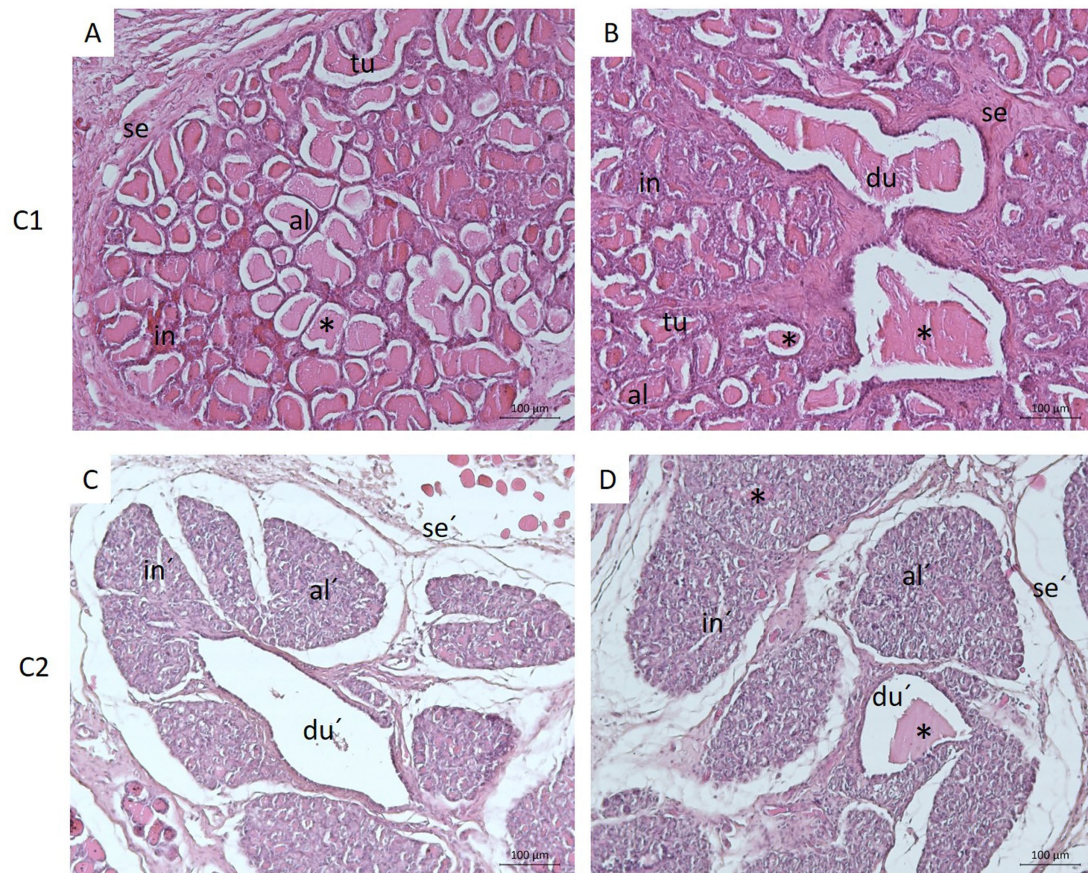


FIGURE 2

Histological structure of the healthy canine mammary gland during active lactation (A,B) and regression (C,D). Panels A and B show well-developed alveoli (al) and tubules (tu) organized within lobules separated by connective tissue septa (se). Alveoli, tubules, and ducts (du) contained secretory product - milk (*). Panels C and D illustrate regressive changes of the glandular tissue manifested by collapsed alveoli (al'), distended interlobular ducts (du') with only occasional occurrence of secretion/milk (*), and expanded connective tissue septa (se') and interstitium (in'). Scale bar: 100 μm , H&E staining.

were highly distended and lined with low, simple cuboidal epithelium. Secretory product was not always found in their lumens. The connective tissue stroma was enlarged (Figures 2C,D).

3.3 Growth curve

3.3.1 Proliferation dynamics assessed by real-time monitoring (xCELLigence system)

The proliferation behavior of primary CMG cells (P1) was evaluated in real time using the xCELLigence system (RTCA), which quantifies the CI as a composite measure of cell number, size, and adhesion. Both CMG cell populations—C1 and C2—demonstrated rapid growth at initial seeding densities of 4,000 and 8,000 cells/well (Figures 3A,B). For C2, increased proliferation was also observed at 2,000 cells/well, though to a lesser extent.

After 48 h, cells at higher densities began to plateau, indicating the onset of contact inhibition. Cultures seeded at 8,000 cells/well reached 80–90% confluence by this time point, after which the CI values slightly declined—suggesting spatial limitations and reduced proliferative activity. In contrast, cells seeded at 4,000 cells/well maintained steady growth between 24 and 72 h,

indicating this density as optimal for further *in vitro* experimentation.

3.3.2 Metabolic activity assessment by XTT assay

To complement real-time proliferation data, metabolic activity of CMG cells (P1) was measured using the XTT assay under identical seeding conditions. As shown in Figures 4A,B, cells seeded at 8,000 cells/well exhibited high metabolic activity within the first 48 h, correlating with the observed early confluence. However, this activity declined thereafter.

Notably, the highest and most sustained metabolic activity over time was recorded in cultures seeded at 4,000 cells/well, corroborating the xCELLigence findings. This concentration supported both robust proliferation and sustained viability, thereby confirming it as the optimal initial seeding density for primary CMG cell culture.

3.4 Immunofluorescence analysis of canine mammary gland cells

Immunofluorescence staining was performed to assess the expression of epithelial, mesenchymal and proliferation markers in

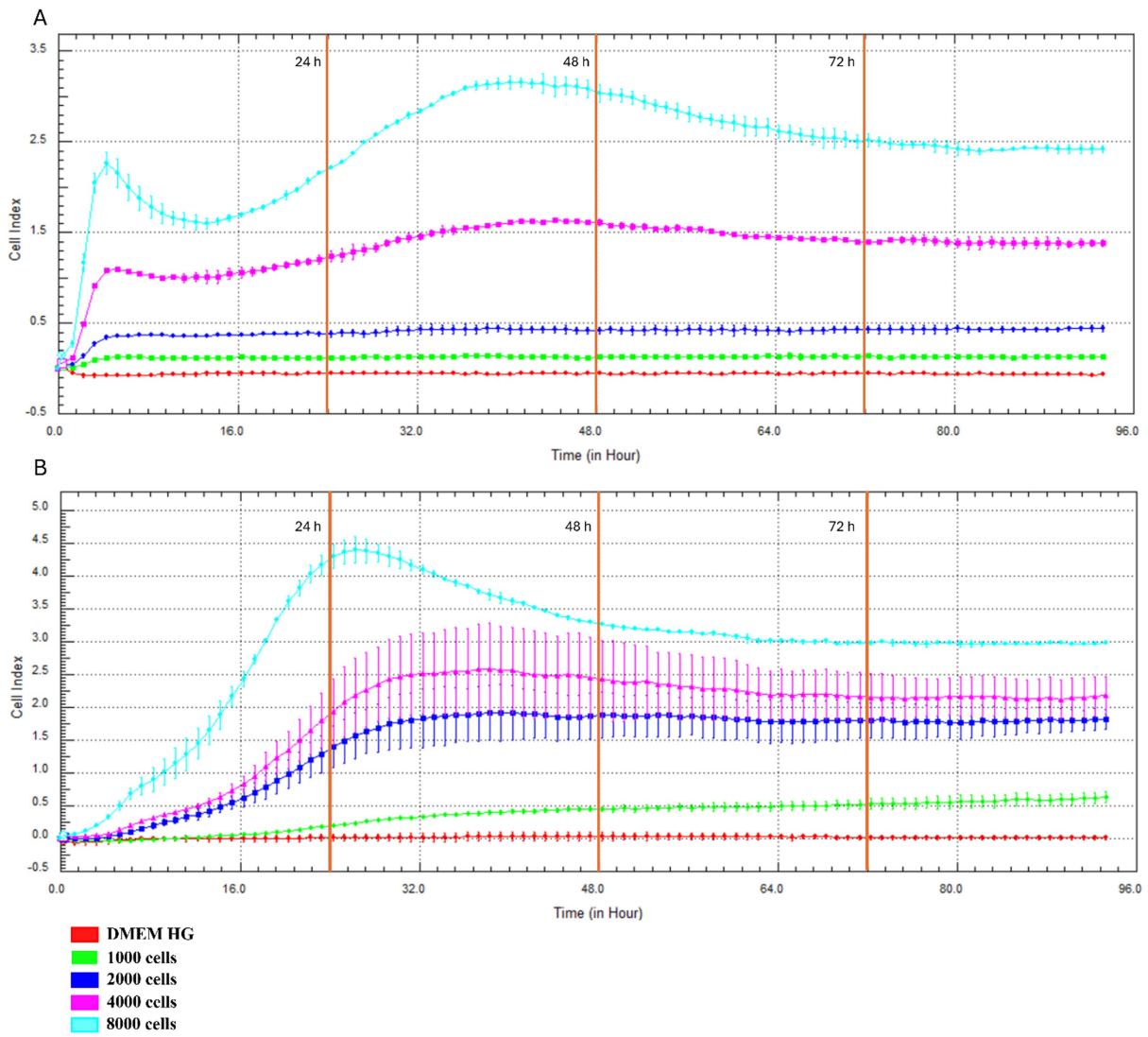


FIGURE 3 Real-time monitoring of CMG cell proliferation using the xCELLigence system. Growth curves of CMG cell populations C1 (A) and C2 (B) seeded at 1,000–8,000 cells/well.

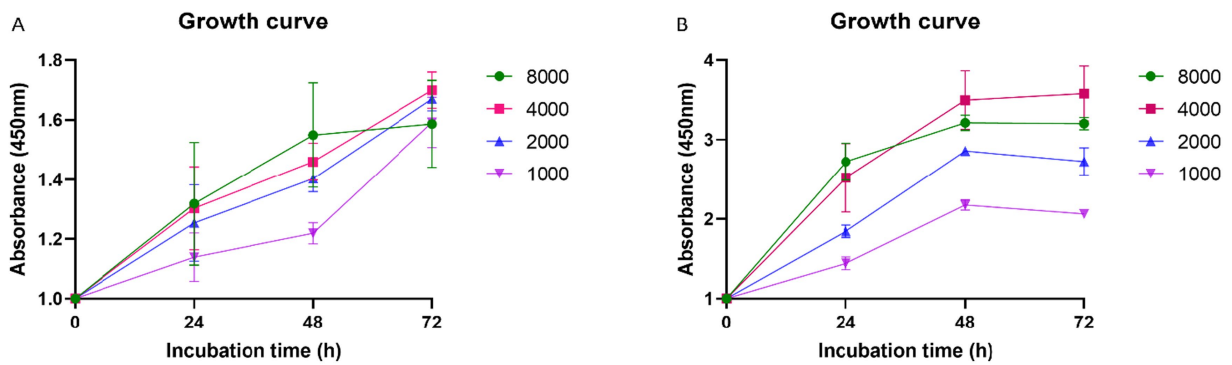


FIGURE 4 Metabolic activity of CMG cells assessed by XTT assay. CMG cell populations C1 (A) and C2 (B) were plated at 1000–8000 cells/well under identical conditions to the xCELLigence assay.

primary CMG cells (P2) and corresponding tissue samples. The evaluated markers included pan-cytokeratin (pan-CK), cytokeratin 8/18 (CK8/18), mucin-1 (MUC1), Ki-67, vimentin and S100. Strong cytoplasmic positivity for pan-CK and CK8/18 was observed in cultured CMG cells, confirming their epithelial origin (Figures 5, 6). These cytokeratins, which are structural components of the intermediate filament cytoskeleton, are widely used to identify luminal epithelial cells in both normal and neoplastic mammary tissue. Expression patterns in cultured cells closely resembled those observed in native mammary gland tissue.

MUC1, a transmembrane glycoprotein involved in epithelial cell protection and adhesion, was abundantly expressed in CMG cells, with apical localization consistent with non-malignant epithelial differentiation (Figure 7).

Analysis of the nuclear proliferation marker Ki-67 revealed low expression levels, indicating a moderate proliferative state in cultured CMG cells (Figure 8). This was consistent with their non-transformed phenotype and supports their relevance as a model for physiologically normal mammary epithelium.

Vimentin is an intermediate filament protein predominantly expressed in mesenchymal cell types. Fibroblasts generally display vimentin intermediate filaments (VIFs) evenly dispersed throughout their cytoplasm (12).

The S100 family comprises calcium-binding proteins involved in cell homeostasis, growth, proliferation, and differentiation, and is associated with cancer progression. S100 proteins are expressed in several cell types including fibroblasts, nerve cells and mammary myoepithelial cells (13–17). Negative expression of both mesenchymal markers, vimentin and S100, was observed in CMG cells (Figures 9, 10). Negative controls showed no specific staining

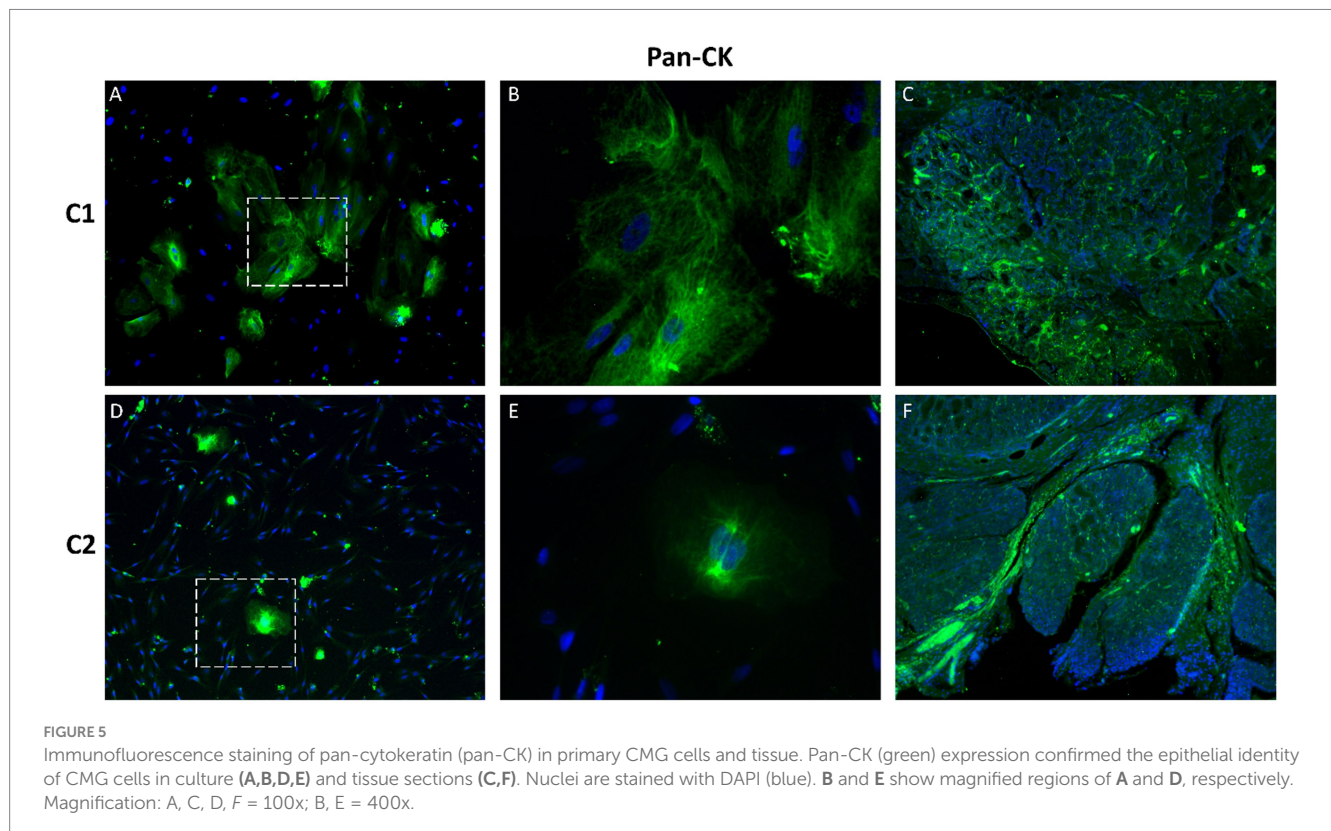
for any of the investigated markers (Supplementary Figures S1–S3).

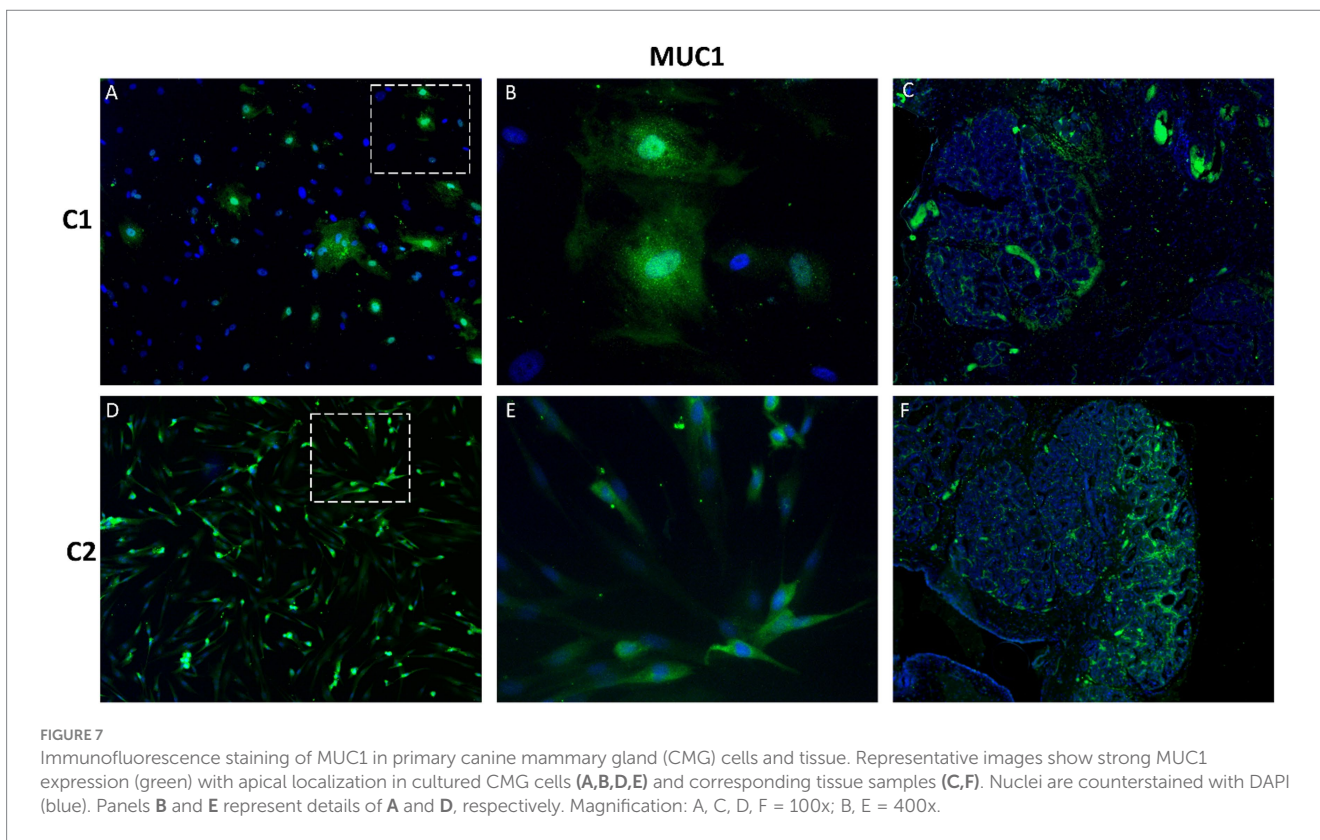
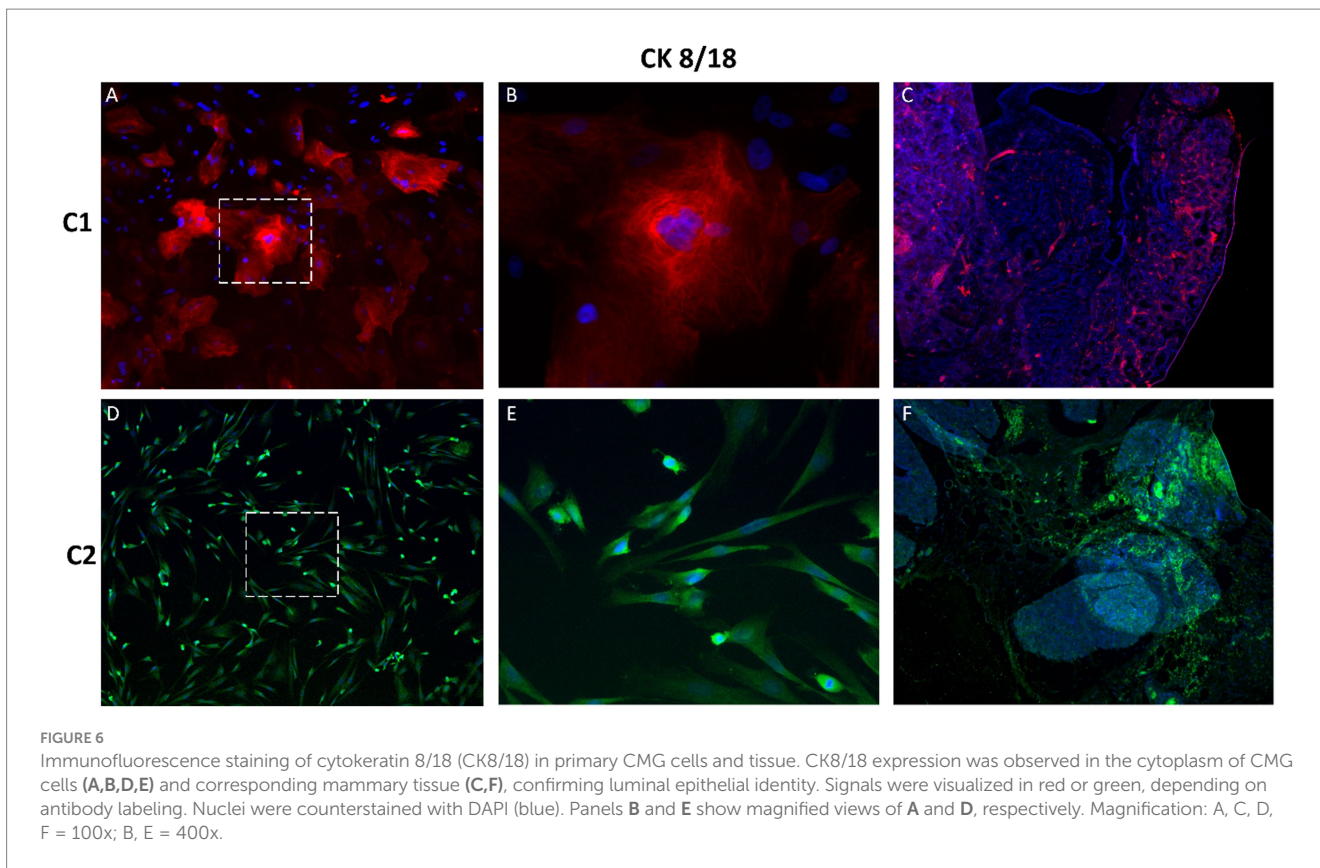
The immunofluorescence panel applied in this study (pan-CK, CK8/18, MUC1, Ki-67, vimentin and S100) consistently showed a luminal epithelial phenotype in cultured CMG cells. We did not detect a distinct cell population with morphological or immunophenotypic features compatible with myoepithelial cells, indicating that the established cultures are luminal-enriched epithelial monolayers.

4 Discussion

The mammary gland, a modified sweat gland, exhibits significant development in females and remains rudimentary in males (18). It is among the few mammalian tissues capable of undergoing cyclical morphological and functional changes - growth, differentiation, and regression - throughout the female's reproductive life, particularly during puberty, pregnancy, lactation, and involution (19). This high degree of hormonal responsiveness renders mammary tissue particularly susceptible to neoplastic transformation (9, 20).

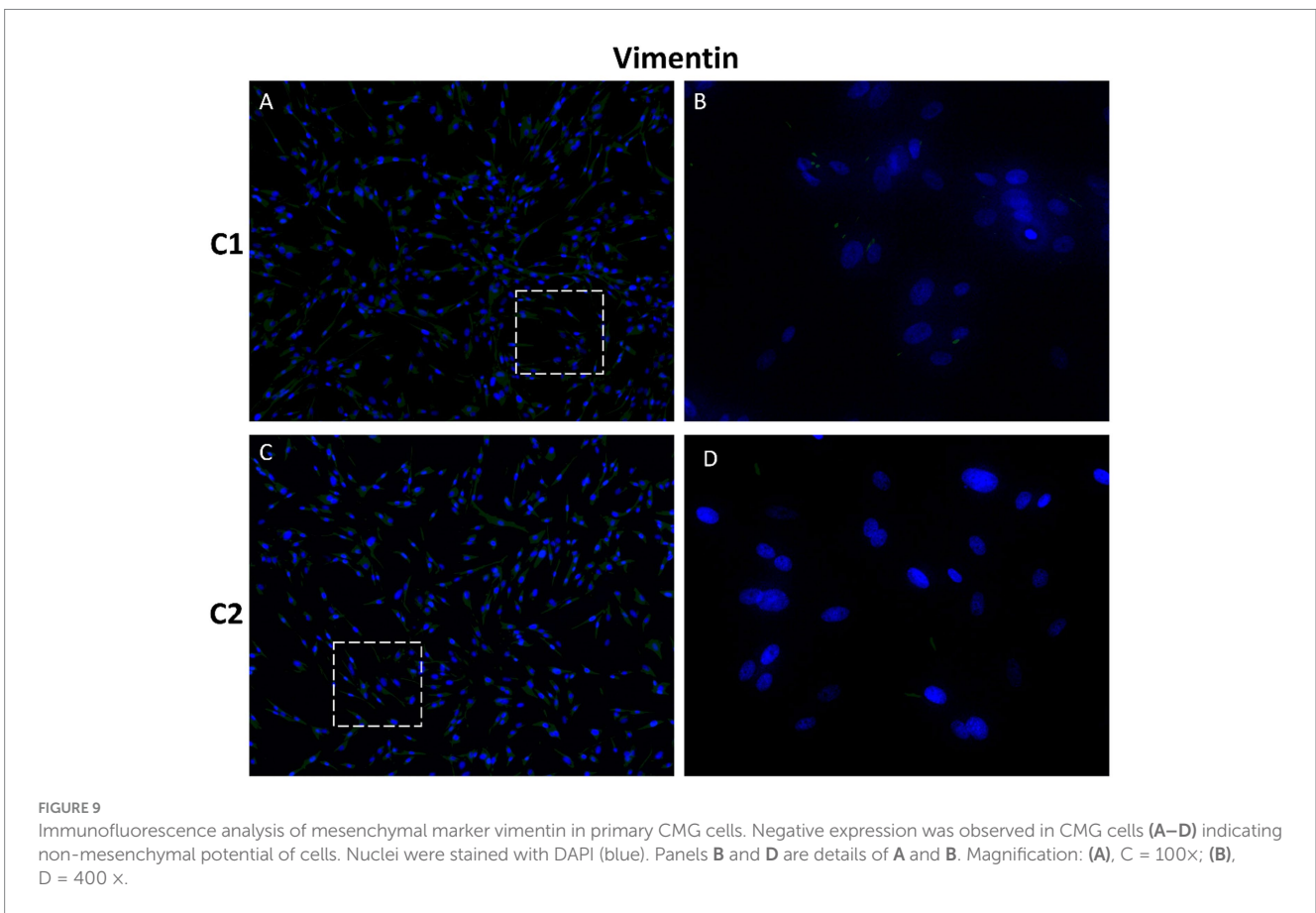
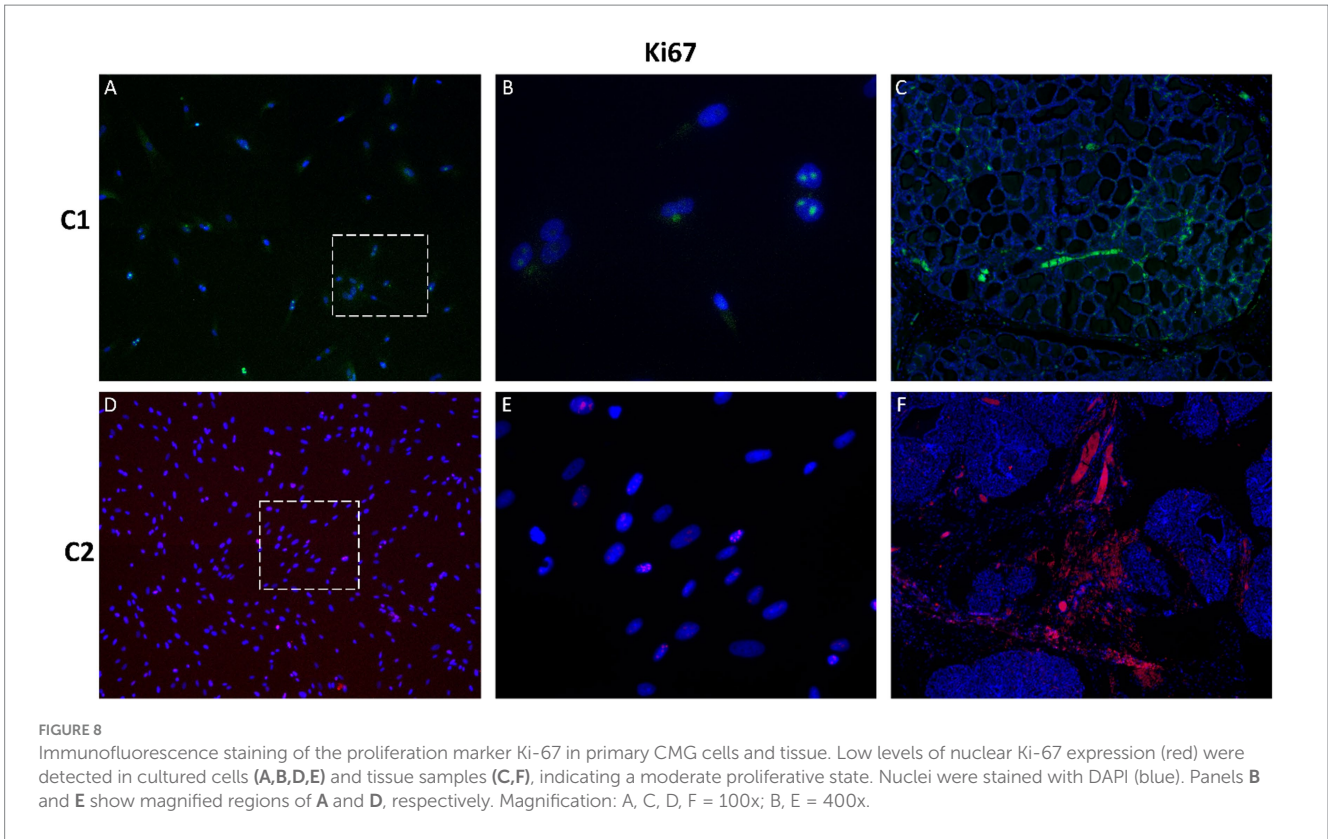
Mammary gland development initiates during embryogenesis with the formation of a rudimentary ductal tree embedded in the mammary fat pad (19). At the onset of puberty, ovarian hormones drive further ductal and alveolar development: estrogen promotes ductal elongation, while progesterone and prolactin orchestrate alveolar morphogenesis (11, 21). During pregnancy, adipose tissue is replaced by glandular epithelium capable of milk secretion. Following weaning, the gland undergoes involution, characterized by apoptosis and extracellular matrix remodeling (22).





Histologically, the active mammary gland comprises secretory alveoli and secretory tubules lined by cuboidal epithelium, supported by myoepithelial cells and a richly vascularized stroma. In contrast,

the inactive gland post-lactation exhibits atrophy, with reduced parenchyma replaced by adipose tissue (23, 24). These phases were evident in our histological analysis (H&E): lactating tissue displayed



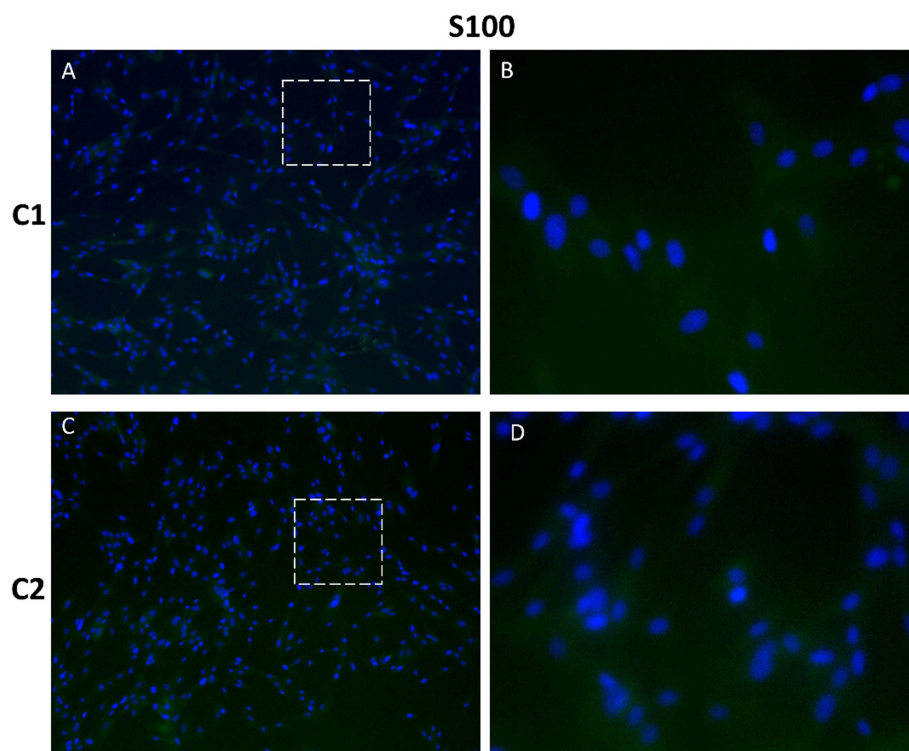


FIGURE 10

Immunofluorescence staining of protein S100 in primary canine mammary cells. Expression of marker S100 was negative in CMG cells (A–D), indicating epithelial luminal origin of cells. Nuclei were counterstained with DAPI (blue). Panels B and D show magnified views of A and C, respectively. Magnification: (A), C = 100 \times ; (B), E = 400 \times .

well-developed alveolar structures, whereas tissue in regression showed disorganized, collapsed alveoli and expanded stromal components, aligning with previously published descriptions of the dynamic remodeling capacity of mammary tissue.

Canine mammary tumors (CMTs) are among the most common neoplasms in intact female dogs, accounting for a significant proportion of tumors in this population, with approximately half exhibiting malignant potential and metastatic behavior (25). Due to significant histopathological, hormonal, and molecular similarities with human BC, including shared oncogenic pathways and hormone responsiveness, CMTs serve as a valuable spontaneous model for translational BC research (26).

Historically, immortalized cell lines have been central to *in vitro* studies on CMTs. While these models offer consistency and scalability, they often fail to replicate the dynamic cellular heterogeneity and microenvironmental interactions of native tissues (27). Additionally, long-term culturing can induce genetic drift, reducing their translational fidelity and clinical relevance (28). These limitations have prompted a shift toward primary cell cultures derived directly from fresh tissue biopsies, which better retain *in vivo* phenotypic characteristics and patient-specific responses.

In our study, we successfully established a two-dimensional primary culture model from healthy CMG tissue using a combined mechanical and enzymatic dissociation protocol. This approach enabled efficient cell isolation, with cells demonstrating robust adherence, rapid proliferation, and confluence within 7 days (29). This methodological choice aligns with protocols employed in previous studies that utilized combined mechanical and enzymatic dissociation

techniques to optimize cell yield and viability in canine mammary tissue (30–32). In contrast (33), reported the successful isolation of primary CMT cells using a mechanical-only method, although this approach may be less efficient for tissues with intact extracellular matrix or limited enzymatic susceptibility.

The efficacy of our combined dissociation method is further supported by the findings of Petroušková et al. (31), who established primary cell cultures from CMG tumors using mechanical disaggregation and enzymatic digestion with type IV collagenase. Their cultures achieved confluency by day 7 and exhibited high expression of epithelial markers along with significant proliferation activity. These results corroborate our observations of rapid cell proliferation and marker expression in primary CMG cultures. Regardless of the technique, published studies consistently report that isolated primary mammary cells - whether from tumor or normal tissue - retain the capacity for proliferation and *in vitro* propagation. Our findings corroborate this, as the CMG cells maintained their proliferative potential across passages, suggesting that our dissociation method preserved cellular integrity and stemness features relevant for subsequent experimentation.

Histological analysis of donor tissue revealed a well-organized lobular structure with active alveoli and ducts, lined by tall cuboidal epithelium and containing lactiferous secretions - features typical of lactating canine mammary glands (34). Similar architecture and epithelial marker expression were reported in tumor-derived cultures (31), supporting the tissue's physiological integrity. By establishing a primary culture from non-neoplastic CMG tissue, we provide a relevant model for studying normal epithelial biology and early

neoplastic changes. This model also offers a benchmark for assessing drug specificity and cytotoxicity, contributing to more accurate preclinical testing and personalized therapy development.

The establishment of primary cell cultures from healthy CMG tissue provides a physiologically relevant model for studying normal mammary function and early neoplastic transformation. To assess proliferative behavior and metabolic activity, we employed the xCELLigence system RTCA and the XTT assay, aiming to define optimal seeding densities for *in vitro* applications. RTCA, which continuously monitors cell proliferation, adhesion, and morphology through electrical impedance, revealed that primary CMG cells seeded at both 4,000 and 8,000 cells/well exhibited rapid early growth, with a clear plateau phase observed after 48 h. However, while 8,000 cells/well resulted in a sharp initial increase in CI due to rapid proliferation and early confluence (80–90%), this was followed by a decline in growth rate, likely driven by spatial constraints and contact inhibition. In contrast, cultures seeded at 4,000 cells/well displayed sustained and linear proliferation over a 24–72 h period, identifying this density as optimal for subsequent *in vitro* experimentation. These findings were corroborated by the XTT assay, which evaluates mitochondrial metabolic activity. CMG cells seeded at 8,000 cells/well showed high metabolic activity only during the first 48 h, after which activity declined, consistent with the plateau and growth inhibition observed in the xCELLigence data. Conversely, cells seeded at 4,000 cells/well maintained higher metabolic activity over a longer duration, supporting their continued viability and proliferative capacity. Together, these data point out the critical importance of optimizing initial seeding density in primary cell cultures to ensure that cells remain in the exponential growth phase. Such standardization enhances reproducibility and reliability in downstream biological and pharmacological assays, particularly in models intended for translational veterinary and comparative oncology research. Our findings align with previous studies using xCELLigence to track proliferation dynamics, such as de Oliveira et al. (51), who used the system to assess glycolysis inhibition in colorectal cancer cells. Likewise, the XTT assay remains a standard for evaluating mitochondrial activity and viability across diverse cell types. Importantly, this study is the first to define optimal seeding density for primary cultures derived from healthy mammary tissue in a 24-well format. In contrast, Petroušková et al. (33) used a lower density (1,000 cells/well) for CMT cultures, reflecting the higher proliferative capacity and altered phenotype of neoplastic cells, which also showed elevated expression of MUC1, CK8/18, and Ki-67. Optimizing growth conditions for healthy CMG cells offers a critical baseline for exploring mammary gland biology, hormonal regulation, and early tumorigenesis. This model also supports the assessment of drug effects on non-malignant cells, key for enhancing therapeutic specificity and safety (35). Ultimately, such cultures contribute to the goals of personalized medicine by replicating normal tissue physiology and advancing both basic and translational veterinary oncology research.

Our immunofluorescence analysis of primary CMG cells revealed robust expression of pan-CK and CK8/18, affirming their epithelial identity (36). Pan-CK antibodies, such as AE1/AE3, target a broad spectrum of cytokeratins, making them effective markers for epithelial cells in both canine and human tissues (37). CK8 and CK18 are intermediate filament proteins characteristic of luminal mammary epithelial cells, and their strong expression in CMG cultures mirrors their localization in normal human breast tissue, indicating a

well-differentiated epithelial phenotype (38, 39). In human BC, the expression patterns of CK8/18 are associated with tumor subtypes and prognoses. Retention of CK8/18 expression correlates with luminal A and B subtypes, which generally have favorable outcomes. Conversely, loss or mislocalization of CK8/18 is linked to basal-like, more aggressive phenotypes (39, 40). Similarly, in canine mammary tumors, benign lesions typically maintain CK8/18 expression, while malignant tumors often exhibit reduced levels, underscoring the role of cytokeratin patterns as indicators of differentiation status (7, 41). However, cytokeratin profiling alone does not provide comprehensive information about proliferative or mesenchymal features. Co-staining with markers such as Ki-67 for proliferation or vimentin for mesenchymal characteristics is necessary to fully characterize growth dynamics and epithelial-mesenchymal transition (42). Moreover, variability in cytokeratin expression due to tissue origin, culture conditions, and passage number highlights the need for standardized protocols to ensure reproducible phenotyping across laboratories (43, 44). Overall, the observed pan-CK and CK8/18 positivity in primary CMG cells aligns with established patterns in human and canine mammary tissues, validating these cultures as models for studying normal epithelial biology and early tumorigenic events (45).

Immunofluorescence analysis of primary CMG cells in our study revealed strong expression of MUC1, a transmembrane glycoprotein integral to epithelial protection and signaling. In normal mammary epithelium, MUC1 is predominantly localized to the apical surface, contributing to the maintenance of cell polarity and forming a protective barrier - an indicator of a well-differentiated state (46, 47). In malignancy, however, MUC1 expression becomes dysregulated. In human BC, MUC1 often shifts from apical to diffuse cytoplasmic or circumferential localization, correlating with loss of cell polarity, invasiveness, and poor prognosis (48, 49). Aberrant glycosylation further enhances MUC1's pro-tumorigenic role, aiding in immune evasion and metastasis (50). Comparable patterns are observed in canine mammary tumors, where normal tissues exhibit apical MUC1 expression, while malignant ones display cytoplasmic redistribution, linked to higher tumor grade and metastatic behavior (51). In our study, CMG cells retained apical MUC1 localization consistent with non-malignant mammary epithelium, highlighting their potential as a pre-neoplastic *in vitro* model. This preserved epithelial phenotype makes them well-suited for investigating early alterations in MUC1 expression and function that may contribute to tumor initiation. Moreover, CMG cultures represent a promising platform for studying the mechanisms of MUC1 dysregulation in cancer progression and for preclinical evaluation of MUC1-targeted therapeutic strategies.

Immunofluorescence staining showed minimal Ki-67 positivity in primary CMG cells, reflecting limited proliferative activity and a predominantly quiescent cellular phenotype. Our finding aligns with the expected profile of non-malignant mammary epithelium, where Ki-67 levels are typically low due to limited mitotic activity. In contrast, elevated Ki-67 expression is a hallmark of CMTs, reflecting their higher proliferative capacity. For instance, Carvalho et al. (52) reported Ki-67 indices ranging from 3 to 32% in benign tumors and 20–49% in malignant ones, correlating with tumor aggressiveness and prognosis. Similarly, in human BC, high Ki-67 expression is associated with increased tumor grade, shorter survival, and higher recurrence risk. A meta-analysis by de

Azambuja et al. (53) confirmed its prognostic value in early-stage BC, demonstrating that Ki-67 positivity confers a higher risk of relapse and worse survival. Furthermore, Luporsi et al. (54) emphasized the predictive relevance of Ki-67 for chemotherapy response, noting that high Ki-67 levels are associated with increased pathological complete response rates in patients undergoing neoadjuvant chemotherapy. The retention of low Ki-67 expression in CMG cultures underscores their utility as a model for studying normal proliferation and early neoplastic changes in both canine and human mammary biology. These cultures provide a relevant platform for investigating the mechanisms underlying Ki-67 dysregulation and its role in tumor progression, offering insights applicable to both veterinary and human oncology.

Immunofluorescence analysis of mesenchymal markers, vimentin and S100, showed negativity for both markers in CMG cells, indicating an epithelial phenotype. Vimentin is typically expressed in cells of mesenchymal origin and regulates cell growth, migration and the maintenance of cellular integrity (12, 55). It has also been associated with cancer invasiveness and increased expression of vimentin was observed in various tumor cells and is considered a marker of epithelial-mesenchymal transition (56, 57). Moreover, vimentin is expressed in the stromal and myoepithelial cell population of the mammary gland (16, 17). The S100 family has many isoforms, and their expression varies by tissue and condition; S100 proteins can be found in fibroblasts, astrocytes, melanocytes, and myoepithelial cells, among others (15, 58–61). Overexpression of some members of S100 family has been reported in several common cancers, including breast cancer (14).

While our findings confirm the epithelial nature and low proliferative activity of CMG cells, certain limitations should be acknowledged. Marker expression was evaluated qualitatively; quantitative techniques such as RNA *in situ* hybridization, as demonstrated by Li et al. (62) for HER2 mRNA in canine mammary tumors, could provide more precise molecular profiling. Our marker panel was limited; inclusion of basal and myoepithelial markers (e.g., CK5, CK14, α -SMA, p63) would allow deeper insight into CMG cell heterogeneity, as these markers are key in distinguishing myoepithelial populations involved in tumor progression (63–65). In the present work, we deliberately focused on establishing a reference luminal epithelial culture from normal CMG tissue and therefore selected a restricted immunofluorescence panel targeting epithelial and luminal markers (pan-CK, CK8/18, MUC1) together with Ki-67 and selected mesenchymal markers (vimentin, S100). Basal/myoepithelial markers (e.g., CK5, CK14, α -SMA, p63) were not included because the available primary material had to be prioritized for initial luminal characterization. Moreover, the dissociation protocol and standard 2D culture conditions used here favor luminal epithelial outgrowth, whereas myoepithelial cells typically require selective enrichment and tailored media to be maintained *in vitro* (29, 65, 66). In line with this, our cultures showed a homogeneous luminal phenotype, and we did not observe an expanding myoepithelial compartment, suggesting that myoepithelial cells from the original tissue did not efficiently proliferate or were gradually lost during early passages. Additionally, the role of MUC1 in normal versus malignant contexts requires further study. While apically localized in healthy tissue, MUC1 becomes mislocalized and aberrantly glycosylated in tumors, contributing to metastasis and immune evasion. Clarifying these

functional shifts could enhance our understanding of mammary gland pathophysiology (67). Future work addressing these aspects will improve the value of CMG cultures as models for mammary biology and tumorigenesis.

5 Conclusion

This study is the first to successfully establish and characterize primary epithelial cell cultures directly from histologically normal CMG tissue, providing a relevant *in vitro* model for studying normal mammary physiology, early tumorigenesis, and supporting future development of standardized control cell lines. Histological analysis confirmed lobular structures typical of actively lactating tissue, validating the functional state of the donor gland. CMG cells adhered efficiently, reached confluence within 7 days, and showed optimal proliferation at 4,000 cells/well, as verified by xCELLigence and XTT assays. These standardized culture conditions offer a practical reference for veterinary laboratories working in diagnostic, pharmacological, or oncological research. Immunofluorescence analysis confirmed epithelial identity (pan-CK, CK8/18), low Ki-67 expression, negative expression of mesenchymal markers (vimentin, S100) and apical MUC1 localization - features indicative of a non-malignant, differentiated phenotype. These data support the use of CMG cultures as a baseline model for distinguishing physiological epithelial characteristics from tumor-associated changes in canine mammary tissue. This model contributes to comparative oncology by enabling more accurate evaluation of tumor biology and therapeutic responses. However, limitations include the qualitative nature of marker assessment and the restricted panel used. Future work should apply quantitative techniques and include additional markers (CK5, CK14, α -SMA, p63), as well as investigate MUC1's role in canine mammary pathology. Overall, CMG cultures provide a valuable platform for translational research and the development of personalized veterinary therapies.

Data availability statement

The original contributions presented in the study are included in the article/[Supplementary material](#), further inquiries can be directed to the corresponding author.

Ethics statement

The animal studies were approved by Ethics committee of the UVMP in Košice (EKVP/2023–02). The studies were conducted in accordance with the local legislation and institutional requirements. Written informed consent was obtained from the owners for the participation of their animals in this study.

Author contributions

NN: Writing – review & editing, Investigation, Writing – original draft, Validation, Data curation, Visualization, Methodology. MH:

Validation, Methodology, Software, Writing – review & editing. AV: Methodology, Writing – review & editing. LH: Methodology, Writing – review & editing, Investigation. BK: Validation, Methodology, Writing – original draft. VA: Writing – original draft, Methodology, Software, Funding acquisition, Data curation. DM: Validation, Methodology, Writing – original draft, Investigation. PK: Writing – original draft, Investigation, Writing – review & editing. SH: Writing – review & editing, Methodology. DC: Visualization, Funding acquisition, Writing – review & editing, Writing – original draft, Conceptualization.

Funding

The author(s) declared that financial support was received for this work and/or its publication. This study was supported by APVV-24-0026 (NN), VEGA 1/0236/23 (VA) and VEGA 1/0122/24 (DC).

Conflict of interest

The author(s) declared that this work was conducted in the absence of any commercial or financial relationships that could be construed as a potential conflict of interest.

References

- Ferreira, T, Gama, A, Seixas, F, Faustino-Rocha, AI, Lopes, C, Gaspar, VM, et al. Mammary glands of women, female dogs and female rats: similarities and differences to be considered in breast Cancer research. *Vet Sci.* (2023) 10:379. doi: 10.3390/vetsci10060379
- Jennings, R, and Premanandan, C. *Veterinary histology*. Ohio: The Ohio State University (2017).
- Abadie, J, Nguyen, F, Loussouarn, D, Peña, L, Gama, A, Rieder, N, et al. Canine invasive mammary carcinomas as models of human breast cancer. Part 2: immunophenotypes and prognostic significance. *Breast Cancer Res Treat.* (2018) 167:459–68. doi: 10.1007/s10549-017-4542-8
- Jedrzejczak-Silicka, M. History of cell culture In: SJ Gowder, editor. *New insights into cell culture technology*. London: IntechOpen (2017)
- Pan, C, Kumar, C, Bohl, S, Klingmueller, U, and Mann, M. Comparative proteomic phenotyping of cell lines and primary cells to assess preservation of cell type-specific functions. *Mol Cell Proteomics.* (2009) 8:443–50. doi: 10.1074/mcp.M800258-MCP200
- Richter, M, Piwocka, O, Musielak, M, Piotrowski, I, Suchorska, WM, and Trzeciak, T. From donor to the lab: a fascinating journey of primary cell lines. *Front Cell Dev Biol.* (2021) 9:381. doi: 10.3389/fcell.2021.711381
- De Faria Lainetti, P, Brandi, A, Leis Filho, AF, Prado, MCM, Kobayashi, PE, Laufer-Amorim, R, et al. Establishment and characterization of canine mammary gland carcinoma cell lines with vasculogenic mimicry ability in vitro and in vivo. *Front Vet Sci.* (2020) 7:583874. doi: 10.3389/fvets.2020.583874
- Inman, JL, Robertson, C, Mott, JD, and Bissell, MJ. Mammary gland development: cell fate specification, stem cells and the microenvironment. *Development.* (2015) 142:1028–42. doi: 10.1242/dev.087643
- Russo, IH, and Russo, J. Mammary gland neoplasia in long-term rodent studies. *Environ Health Perspect.* (1996) 104:938–67. doi: 10.1289/ehp.96104938
- Stefanowicz-Hajduk, J, and Ochocka, JR. Real-time cell analysis system in cytotoxicity applications: usefulness and comparison with tetrazolium salt assays. *Toxicol Rep.* (2020) 7:335–44. doi: 10.1016/j.toxrep.2020.02.002
- Javed, A, and Lteif, A. Development of the human breast. *Semin Plast Surg.* (2013) 27:005–12. doi: 10.1055/s-0033-1343989
- Miron-Mendoza, M, Poole, K, DiCesare, S, Nakahara, E, Bhatt, MP, Hulleman, JD, et al. The role of vimentin in human corneal fibroblast spreading and myofibroblast transformation. *Cells.* (2024) 13:1094. doi: 10.3390/cells13131094

Generative AI statement

The author(s) declared that Generative AI was not used in the creation of this manuscript.

Any alternative text (alt text) provided alongside figures in this article has been generated by Frontiers with the support of artificial intelligence and reasonable efforts have been made to ensure accuracy, including review by the authors wherever possible. If you identify any issues, please contact us.

Publisher's note

All claims expressed in this article are solely those of the authors and do not necessarily represent those of their affiliated organizations, or those of the publisher, the editors and the reviewers. Any product that may be evaluated in this article, or claim that may be made by its manufacturer, is not guaranteed or endorsed by the publisher.

Supplementary material

The Supplementary material for this article can be found online at: <https://www.frontiersin.org/articles/10.3389/fvets.2025.1652991/full#supplementary-material>

- Zimmer, DB, Cornwall, EH, Landar, A, and Song, W. The S100 protein family: history, function, and expression. *Brain Res Bull.* (1995) 37:417–29. doi: 10.1016/0361-9230(95)00040-2
- Cross, SS, Hamdy, FC, Deloulme, JC, and Rehman, I. Expression of S100 proteins in normal human tissues and common cancers using tissue microarrays: S100A6, S100A8, S100A9 and S100A11 are all overexpressed in common cancers. *Histopathology.* (2005) 46:256–69. doi: 10.1111/j.1365-2559.2005.02097.x
- Tomcik, M, Palumbo-Zerr, K, Zerr, P, Avouac, J, Dees, C, Sumova, B, et al. S100A4 amplifies TGF- β -induced fibroblast activation in systemic sclerosis. *Ann Rheum Dis.* (2015) 74:1748–55. doi: 10.1136/annrheumdis-2013-204516
- Peuhu, E, Virtakoivu, R, Mai, A, Wärrä, A, and Ivaska, J. Epithelial vimentin plays a functional role in mammary gland development. *Development.* (2017) 144:4103–13. doi: 10.1242/dev.154229
- Finot, L, Chanut, E, and Dessauge, F. Molecular signature of the putative stem/progenitor cells committed to the development of the bovine mammary gland at puberty. *Sci Rep.* (2018) 8:16194. doi: 10.1038/s41598-018-34691-2
- Khan, YS, Fakoya, AO, and Sajjad, H. *Anatomy, thorax: mammary gland*. Treasure Island, FL: StatPearls Publishing (2025).
- Biswas, SK, Banerjee, S, Baker, GW, Kuo, C-Y, and Chowdhury, I. The mammary gland: basic structure and molecular Signaling during development. *Int J Mol Sci.* (2022) 23:3883. doi: 10.3390/ijms23073883
- Macias, H, and Hinck, L. Mammary gland development. *Wiley Interdiscip Rev Dev Biol.* (2012) 1:533–57. doi: 10.1002/wdev.35
- Oakes, SR, Rogers, RL, Naylor, MJ, and Ormandy, CJ. Prolactin regulation of mammary gland development. *J Mammary Gland Biol Neoplasia.* (2008) 13:13–28. doi: 10.1007/s10911-008-9069-5
- Monks, NR, Cherba, DM, Kamerling, SG, Simpson, H, Rusk, AW, Carter, D, et al. A multi-site feasibility study for personalized medicine in canines with osteosarcoma. *J Transl Med.* (2013) 11:158. doi: 10.1186/1479-5876-11-158
- Sorenmo, KU, Rasotto, R, Zappulli, V, and Goldschmidt, MH. Development, anatomy, histology, lymphatic drainage, clinical features, and cell differentiation markers of canine mammary gland neoplasms. *Vet Pathol.* (2011) 48:85–97. doi: 10.1177/0300985810389480
- Watson, CJ. Key stages in mammary gland development - involution: apoptosis and tissue remodelling that convert the mammary gland from milk factory to a quiescent organ. *Breast Cancer Res.* (2006) 8:203. doi: 10.1186/bcr1401

25. Moe, L. Population-based incidence of mammary tumours in some dog breeds. *J Reprod Fertil Suppl.* (2001) 57:439–43.
26. Vilhena, H, Figueira, AC, Schmitt, F, Canadas, A, Chaves, R, Gama, A, et al. Canine and feline spontaneous mammary tumours as models of human breast Cancer In: MR Pastorinho and ACA Sousa, editors. Cham: Springer International Publishing (2020). 173–207.
27. Nowak, E, Krajewski, W, Malkiewicz, B, Szydelko, T, and Pawlak, A. Characteristics and applications of canine in vitro models of bladder Cancer in veterinary medicine: an up-to-date Mini review. *Animals.* (2022) 12:516. doi: 10.3390/ani12040516
28. Schilsky, RL. Personalized medicine in oncology: the future is now. *Nat Rev Drug Discov.* (2010) 9:363–6. doi: 10.1038/nrd3181
29. Sánchez-Céspedes, R, Maniscalco, L, Iussich, S, Martignani, E, Guil-Luna, S, De Maria, R, et al. Isolation, purification, culture and characterisation of myoepithelial cells from normal and neoplastic canine mammary glands using a magnetic-activated cell sorting separation system. *Vet J.* (2013) 197:474–82. doi: 10.1016/j.tvjl.2013.03.005
30. Cocola, C, Anastasi, P, Astigiano, S, Piscitelli, E, Pelucchi, P, Vildardo, L, et al. Isolation of canine mammary cells with stem cell properties and tumour-initiating potential. *Reprod Domest Anim.* (2009) 44:214–7. doi: 10.1111/j.1439-0531.2009.01413.x
31. Petroušková, P, Hudáková, N, Almášiová, V, Valenčáková, A, Hornáková, L, Huniadi, M, et al. Establishment of primary cell cultures from canine mammary gland malignant tumours: a preliminary study. *J Vet Res.* (2025) 69:159–68. doi: 10.2478/jvetres-2025-0007
32. Zamani-Ahmadmahmudi, M, Nassiri, SM, Jahanzad, I, Shirani, D, Rahbarghazi, R, and Yazdani, B. Isolation and characterization of a canine mammary cell line prepared for proteomics analysis. *Tissue Cell.* (2013) 45:183–90. doi: 10.1016/j.tice.2012.11.002
33. Ardicli, S, Samli, H, Mecitoglu, G, Vatanserver, B, and Mutlu, AM. The establishment of primary cell culture from canine mammary gland tumor. *J Cell Biotechnol.* (2021) 7:57–65. doi: 10.3233/JCB-210036
34. Orfanou, DC, Poulris, A, Ververidis, HN, Mavrogiani, VS, Taitzoglou, IA, Boscos, CM, et al. Histological features in the mammary glands of female dogs throughout lactation. *Anat Histol Embryol.* (2010) 39:473–8. doi: 10.1111/j.1439-0264.2010.01018.x
35. Caceres, S, Peña, L, de Andres, PJ, Illera, MJ, Lopez, MS, Woodward, WA, et al. Establishment and characterization of a new cell line of canine inflammatory mammary cancer: IPC-366. *PLoS One.* (2015) 10:e0122277. doi: 10.1371/journal.pone.0122277
36. Barak, V, Goike, H, Panaretakis, KW, and Einarsson, R. Clinical utility of cytokeratins as tumor markers. *Clin Biochem.* (2004) 37:529–40. doi: 10.1016/j.clinbiochem.2004.05.009
37. Menz, A, Gorbokov, N, Viehweger, F, Lennartz, M, Hube-Magg, C, Hornsteiner, L, et al. Pan-keratin immunostaining in human Tumors: a tissue microarray study of 15,940 Tumors. *Int J Surg Pathol.* (2023) 31:927–38. doi: 10.1177/10668969221117243
38. Abd El-Rehim, DM, Pinder, SE, Paish, CE, Bell, J, Blamey, RW, Robertson, JFR, et al. Expression of luminal and basal cytokeratins in human breast carcinoma. *J Pathol.* (2004) 203:661–71. doi: 10.1002/path.1559
39. Aiad, HA, Samaka, RM, Asaad, NY, Kandil, MA, Shehata, MA, and Miligy, IM. Relationship of CK8/18 expression pattern to breast cancer immunohistochemical subtyping in Egyptian patients. *Ecancermedicalscience.* (2014) 8:404. doi: 10.3333/ecancer.2014.404
40. Amirkhani Namagerdi, A, d'Angelo, D, Ciani, F, Iannuzzi, CA, Napolitano, F, Avallone, L, et al. Triple-negative breast Cancer comparison with canine mammary Tumors from light microscopy to molecular pathology. *Front Oncol.* (2020) 10:563779. doi: 10.3389/fonc.2020.563779
41. Fhaikrue, I, Srisawat, W, Nambooppha, B, Pringproa, K, Thongtharb, A, Prachasilchai, W, et al. Identification of potential canine mammary tumour cell biomarkers using proteomic approach: differences in protein profiles among tumour and normal mammary epithelial cells by two-dimensional electrophoresis-based mass spectrometry. *Vet Comp Oncol.* (2020) 18:787–95. doi: 10.1111/vco.12610
42. Sammarco, A, Gomiero, C, Beffagna, G, Cavicchioli, L, Ferro, S, Michieletto, S, et al. Epithelial-to-mesenchymal transition and phenotypic marker evaluation in human, canine, and feline mammary gland Tumors. *Animals (Basel).* (2023) 13:878. doi: 10.3390/ani13050878
43. Paladino, G, Marino, C, La Terra, MS, Civile, C, Rusciano, D, and Enea, V. Cytokeratin expression in primary epithelial cell culture from bovine conjunctiva. *Tissue Cell.* (2004) 36:323–32. doi: 10.1016/j.tice.2004.05.003
44. Sidney, LE, McIntosh, OD, and Hopkinson, A. Phenotypic change and induction of cytokeratin expression during in vitro culture of corneal stromal cells. *Invest Ophthalmol Vis Sci.* (2015) 56:7225–35. doi: 10.1167/iovs.15-17810
45. Oakes, SR, Gallego-Ortega, D, and Ormandy, CJ. The mammary cellular hierarchy and breast cancer. *Cell Mol Life Sci.* (2014) 71:4301–24. doi: 10.1007/s00018-014-1674-4
46. Brayman, M, Thatiah, A, and Carson, DD. MUC1: a multifunctional cell surface component of reproductive tissue epithelia. *Reprod Biol Endocrinol.* (2004) 2:4. doi: 10.1186/1477-7827-2-4
47. Semba, R, Horimoto, Y, Sakata-Matsuzawa, M, Ishizuka, Y, Denda-Nagai, K, Fujihira, H, et al. Possible correlation of apical localization of MUC1 glycoprotein with luminal A-like status of breast cancer. *Sci Rep.* (2023) 13:5281. doi: 10.1038/s41598-023-32579-4
48. Joshi, S, Kumar, S, Choudhury, A, Ponnusamy, MP, and Batra, SK. Altered mucins (MUC) trafficking in benign and malignant conditions. *Oncotarget.* (2014) 5:7272–84. doi: 10.18632/oncotarget.2370
49. Li, Q, Chu, Y, Li, S, Yu, L, Deng, H, Liao, C, et al. The oncoprotein MUC1 facilitates breast cancer progression by promoting Pink1-dependent mitophagy via ATAD3A destabilization. *Cell Death Dis.* (2022) 13:899–16. doi: 10.1038/s41419-022-05345-z
50. Chen, X, Sandrine, IK, Yang, M, Tu, J, and Yuan, X. MUC1 and MUC16: critical for immune modulation in cancer therapeutics. *Front Immunol.* (2024) 15:913. doi: 10.3389/fimmu.2024.1356913
51. de Oliveira, JT, Pinho, SS, de Matos, AJ, Hespanhol, V, Reis, CA, and Gärtner, F. MUC1 expression in canine malignant mammary tumours and relationship to clinicopathological features. *Vet J.* (2009) 182:491–3. doi: 10.1016/j.tvjl.2008.09.007
52. Carvalho, MI, Pires, I, Prada, J, Lobo, L, and Queiroga, FL. Ki-67 and PCNA expression in canine mammary Tumors and adjacent nonneoplastic mammary glands: prognostic impact by a multivariate survival analysis. *Vet Pathol.* (2016) 53:1138–46. doi: 10.1177/0300985816646429
53. De Azambuja, E, Cardoso, F, de Castro, G, Colozza, M, Mano, MS, Durbecq, V, et al. Ki-67 as prognostic marker in early breast cancer: a meta-analysis of published studies involving 12,155 patients. *Br J Cancer.* (2007) 96:1504–13. doi: 10.1038/sj.bjc.6603756
54. Luporsi, E, André, F, Spyrtos, F, Martin, P-M, Jacquemier, J, Penault-Llorca, F, et al. Ki-67: level of evidence and methodological considerations for its role in the clinical management of breast cancer: analytical and critical review. *Breast Cancer Res Treat.* (2012) 132:895–915. doi: 10.1007/s10549-011-1837-z
55. Surolija, R, Li, FJ, Wang, Z, Li, H, Dsouza, K, Thomas, V, et al. Vimentin intermediate filament assembly regulates fibroblast invasion in fibrogenic lung injury. *JCI Insight.* (2019) 4:e123253. doi: 10.1172/jci.insight.123253
56. Yamashita, N, Tokunaga, E, Kitao, H, Hisamatsu, Y, Taketani, K, Akiyoshi, S, et al. Vimentin as a poor prognostic factor for triple-negative breast cancer. *J Cancer Res Clin Oncol.* (2013) 139:739–46. doi: 10.1007/s00432-013-1376-6
57. Kokkinos, MI, Wafai, R, Wong, MK, Newgreen, DF, Thompson, EW, and Waltham, M. Vimentin and epithelial-mesenchymal transition in human breast Cancer – observations in vitro and in vivo. *Cells Tissues Organs.* (2007) 185:191–203. doi: 10.1159/000101320
58. Du, J, Yi, M, Zhou, F, He, W, Yang, A, Qiu, M, et al. S100B is selectively expressed by gray matter protoplasmic astrocytes and myelinating oligodendrocytes in the developing CNS. *Mol Brain.* (2021) 14:154. doi: 10.1186/s13041-021-00865-9
59. Petersson, S, Shubbar, E, Enerbäck, L, and Enerbäck, C. Expression patterns of S100 proteins in melanocytes and melanocytic lesions. *Melanoma Res.* (2009) 19:215–25. doi: 10.1097/CMR.0b013e32832c6358
60. Baudier, J, and Gentil, BJ. The S100B protein and Partners in Adipocyte Response to cold stress and adaptive thermogenesis: facts, hypotheses, and perspectives. *Biomolecules.* (2020) 10:843. doi: 10.3390/biom10060843
61. Popnikolov, NK, Ayala, AG, Graves, K, and Gatalica, Z. Benign myoepithelial tumors of the breast have immunophenotypic characteristics similar to metaplastic matrix-producing and spindle cell carcinomas. *Am J Clin Pathol.* (2003) 120:161–7. doi: 10.1309/G6CT-R8MD-TFUW-19XV
62. Li, R, Wu, H, Sun, Y, Zhu, J, Tang, J, Kuang, Y, et al. A novel canine mammary Cancer cell line: preliminary identification and utilization for drug screening studies. *Front Vet Sci.* (2021) 8:906. doi: 10.3389/fvets.2021.665906
63. Deckwirth, V, Rajakylä, EK, Cattavarayane, S, Acheva, A, Schaible, N, Krishnan, R, et al. Cytokeratin 5 determines maturation of the mammary myoepithelium. *iScience.* (2021) 24:102413. doi: 10.1016/j.isci.2021.102413
64. Gärtner, F. p63: a novel myoepithelial cell marker in canine mammary tissues. *Vet Pathol.* (2003) 40:412–20. doi: 10.1354/VP.40-4-412
65. Sánchez-Céspedes, R, Millán, Y, Guil-Luna, S, Reymundo, C, de Espinosa los Monteros, A, and Martín las Mulas, J. Myoepithelial cells in canine mammary tumours. *Vet J.* (2016) 207:45–52. doi: 10.1016/j.tvjl.2015.10.035
66. Zubeldia-Plazaola, A, Ametller, E, Mancino, M, de Prats Puig, M, López-Plana, A, Guzman, F, et al. Comparison of methods for the isolation of human breast epithelial and myoepithelial cells. *Front Cell Dev Biol.* (2015) 3:32. doi: 10.3389/fcell.2015.00032
67. Rajakylä, K, Krishnan, R, and Tojkander, S. Analysis of contractility and invasion potential of two canine mammary tumor cell lines. *Front Vet Sci.* (2017) 4:149. doi: 10.3389/fvets.2017.00149